21, rue d'Artois, F-75008 PARIS
http : //www.cigre.org

CIGRE US National Committee
2023 Grid of the Future Symposium

Testing and Characterization of Fault Scenarios of a Hierarchical DC Microgrid for Residential Applications

Andrew R. R. DOW, Matthew J. RENO, Miguel JIMENEZ-APARICIO
Sandia National Laboratories
USA

Daniel BAUER, Daniel RUIZ, Brian WARD
BlockEnergy, subsidiary of Emera Technologies
Canada

SUMMARY

Electrical faults within power distribution systems can have serious effects on local communities and environments resulting in fire damages to property and wildlife, severe financial losses, and worst of all, loss of life. Failures to electrical distribution systems are the third leading cause of home structure fires with the U.S. seeing more than 28,000 fires and $700 million in property damage each year [1]. A better understanding of the behavior during an electrical fault event can lead to faster and safer detection prior to these catastrophic outcomes. The testing and characterization of electrical faults on a microgrid are studied in this paper to understand the effects these can have on a distributed power system. A direct current (DC) microgrid residing on Kirtland Airforce Base in Albuquerque, NM serves as an experimental testing platform for introducing controlled line faults to study the electrical behavior of the system. The microgrid is part of a cooperative research and development agreement (CRADA) between Sandia National Laboratories and Emera Technologies to study the application of DC power distribution between residential housing, utility services, and laboratory facilities focusing on distributed energy resource (DER) research [2]. A key component of the research being pursued with this microgrid platform is the study of electrical faults for faster detection and a better understanding of fault behavior on the entire power system. While previously published work on the subject focuses on experimental fault testing on a laboratory-based DC microgrid [3-6], the KAFB microgrid offers a development platform that is a functioning power distribution network for residential load service to end-users. This development platform bridges the gap between development of fault detection research and integration into commercial distribution systems.

This paper details the architecture of the DC microgrid; a hierarchical system that relies on a distributed network of nanogrids and a central control unit to implement coordinated power

ardow@sandia.gov

sharing between residential loads and interconnection to the local utility grid. Fault protection is enabled on the microgrid in the form of a supervisory protection hardware that monitors the distribution bus for electrical fault signatures. An emulated fault test setup is introduced into the microgrid to observe how the microgrid reacts to various fault events initiated onto the distribution bus. The fault emulator can be varied in fault impedance and type, installed location, and tested under different bus topologies. As different faults are experimentally tested, transient current and voltage waveforms are captured to identify potential risks and outcomes during the fault events. This characterization of electrical faults allows for further research into the protection and detection methods with the intent of creating more resilient power distribution systems against fault scenarios.

KEYWORDS

DC microgrid, electrical faults, distributed energy resources, power distribution, fault detection

DC MICROGRID ARCHITECTURE

The Kirtland Airforce Base (KAFB) DC Microgrid has been developed and deployed to support residential power service applications since 2019 [2]. The microgrid serves ten end-user nodes, including housing and laundry facilities and doubling as a development testbed for DC microgrid applications at Sandia National Laboratories' Distributed Energy Technology Laboratory (DETL). Fig. 1 contains a map of the entire KAFB microgrid, spanning approximately 1.5 kilometers in distribution bus length. Some research conducted thus far on the microgrid includes fault detection and exploring alternative microgrid bus topologies to increase resiliency and reliability to the microgrid. The microgrid is made up of a series of interconnected nanogrid boxes, each serving individual housing loads. Each nanogrid features a battery energy storage component, interface converter for rooftop photovoltaic (PV) solar, grid-forming inverter for residential AC loads, and a transfer switch connecting to a local utility AC grid. In the event of the DC microgrid being disabled, the transfer switch provides interrupted service to the housing loads from the utility grid. During typical operation, the microgrid is self-sufficient to the end-user, generating enough power through its PV resources to support AC loads and maintain energy storage charge [7].

The nanogrid units are connected to the hierarchical microgrid network using a 750 V distribution bus, ground-centered to allow for a ±375 V bipolar distribution bus. This bipolar bus configuration contains a high-impedance grounding scheme in which current flows through the positive and negative poles rather than through the distribution bus ground. Lower overall bus operating voltages with respect to ground are achieved as well as less severe risks associated with ground fault scenarios. Each nanogrid relies on a bidirectional interface converter to allow for power flow between its internal DC voltage node and the microgrid's distribution bus. Depending on the nanogrid source generation and load demand, power is transferred between nanogrids through the distribution bus as part of the overall microgrid operation. The bidirectional interface converter for each of the nanogrids limits the current provided to and from the nanogrid box, limiting high current peaks found in low-impedance fault conditions from the internal energy storage component. Fig. 2 outlines the overall architecture of the nanogrid boxes serving each end-user.

Fig. 1. KAFB DC microgrid serving housing, utility, and DETL sites.

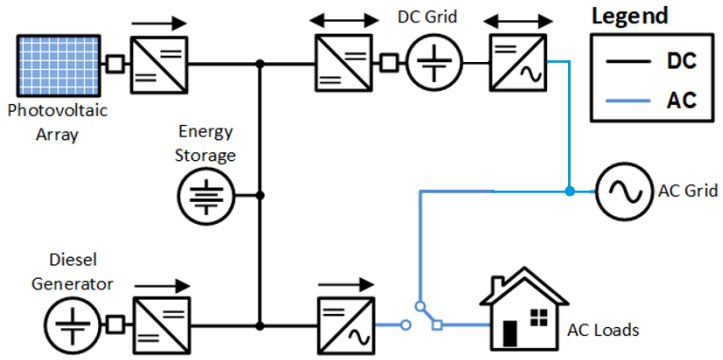

Fig. 2. BlockBox nanogrid architecture showing integration of DERs into residential application [7].

Another key component of the DC microgrid architecture is the Central Energy Park (CEP), acting as the microgrid's hierarchical bus controller. The CEP sets the microgrid distribution voltage and interfaces to the local utility grid through a DC/AC grid-following inverter that allows for bidirectional power flow. Power can be imported/exported between the microgrid and utility based on the generation and demand within the system, notably during the loss of PV power, surplus in generated PV power, and black start conditions. Each of the nanogrid boxes are networked to the CEP, located at the KAFB's laundry facility to allow for coordinated power control in the system. The CEP contains its own power generation in the form of a local battery energy source, PV solar array field, and backup natural gas generators.

The CEP also serves an important function of protecting the microgrid in the event of faults and transients found on the microgrid bus. First, a high-impedance grounding scheme allows the ground of the system to float between parallel RC networks placed between the bipolar rails. This circuit provides a high-frequency return path while maintaining high-impedance for DC, ensuring that bus current flows between the positive and negative rails and not through the system ground. This is shown in Fig. 3a. Furthermore, a protection device located at the CEP continuously monitors the current from the CEP's node on the microgrid to determine if a fault has occurred. Detecting a fault on the microgrid distribution bus, the protection device can be enabled to immediately disconnect the sourced 750 V and clamp the line to a low impedance, removing any potential voltage or current from being a safety risk to the end user and equipment [8]. When a fault event occurs and the protection device is enabled, each of the nanogrid boxes continues to operate in an islanded configuration. Furthermore, the microgrid bus being disabled removes the fault from affecting the AC utility grid connected through the grid-feeding inverter tie at the CEP. Islanding both the nanogrid boxes and the utility grid allows for the fault to be detected and removed without interrupting service to the end user or affecting utility service outside of the microgrid. Upon the removal of a fault, the microgrid bus can be enabled by coordinating control from the CEP. This is detailed in Fig. 3b.

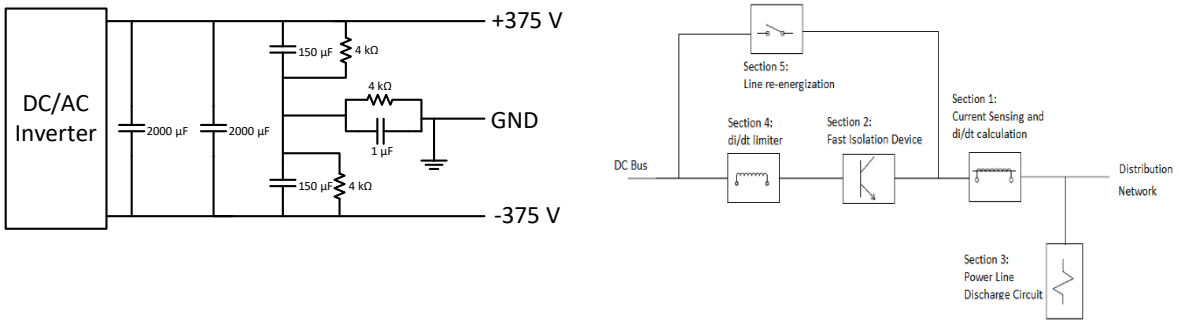

(a) *(b)*

Fig. 3. (a) High-impedance grounding scheme found at CEP and (b) protection device used to detect and disable faults [8].

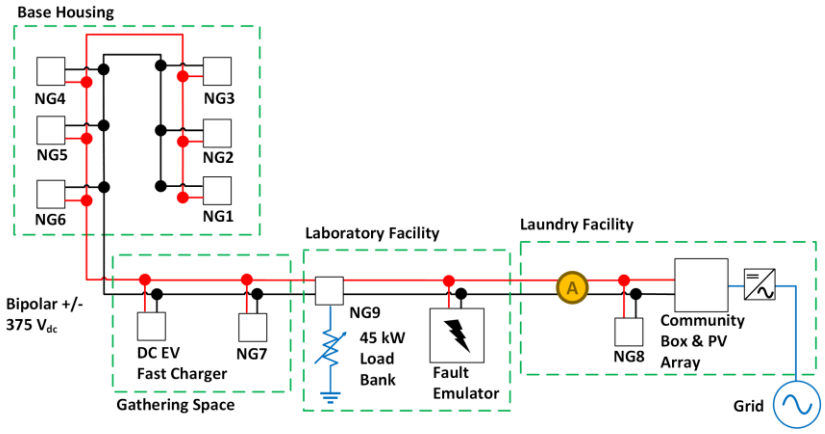

Fig. 4. KAFB microgrid architecture in a radial feed bus configuration.

The KAFB DC microgrid allows for different bus topologies. Two feeds exist between the CEP and the distribution bus connecting each of the ten nanogrid boxes. Through a network of disconnect switches, either radial feeds or a loop feed can be configured for the distribution network. The loop feed advances the distribution capability and redundancy of the system, allowing for power to optimally flow through the system based on nanogrid location. Fig. 4 and Fig. 5 identify two possible bus topologies for the microgrid: a radial feed between the CEP (titled Community Box) and base housing or a loop feed that connects directly between the CEP and base housing.

Faults can be a common occurrence in power distribution applications and need to be fully understood for every system. Whether the faults are introduced through catastrophic weather events, improper installation, or equipment malfunction, it is important to create a controlled environment, in which faults can be tested and characterized within the power system. Without fully characterizing and understanding the effects of faults on a power distribution bus, potential hazards exist when a fault event occurs. Loss of life, destruction of property, and interrupted service are all real examples of how faults in power networks can have a negative impact on the surrounding community [1]. For DC microgrids, a relatively new concept in power distribution applications [9], capturing the effects of faults on a system and methods for detecting and protecting against system faults can help develop the technology and solutions that will avoid harm and impact [10-13]. In the case of the KAFB DC microgrid, a method for emulating faults to the distribution bus is further examined. Introducing faults onto the system and studying the behavior of nanogrid boxes, the CEP, and its protection device using multiple bus topologies is outlined in the coming sections.

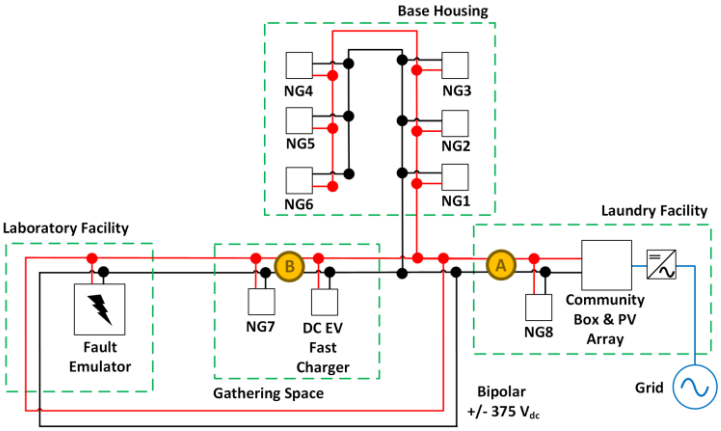

Fig. 5. KAFB microgrid architecture in a loop feed bus configuration.

EXPERIMENTAL FAULT TEST SETUP

The test method aims to introduce electrical faults on the power distribution bus of the KAFB DC microgrid in a controlled manner, allowing for the characterization of the fault signatures at multiple fault locations, measured locations, and with varying fault types. The type of faults focused on during this test are typically low-impedance connections between the distribution bus voltage and high-impedance ground or connections between the two bipolar distribution bus voltages. As one can imagine, a low-impedance connection between high potential nets can lead to high transients in current and voltage due to the instantaneous flow of current through the fault connection. This behavior is expected but will be captured fully through a fault emulation setup configurable on the KAFB microgrid.

Emulated faults can be introduced onto the KAFB DC microgrid using a hardware device connected to the main distribution bus. The fault emulator hardware consists of a series/parallel bank of power resistors with total impedance value configurable between 1 Ω and 1000 Ω. An electromechanical contactor switch manually initiates and clears the fault introduced onto the bus for a duration of time long enough to capture the transient effects of the fault. Further configurable, either line voltage to ground or line voltage to line voltage scenarios can be set up, introducing a multitude of positive, negative, and ground-based impedance faults onto the system.

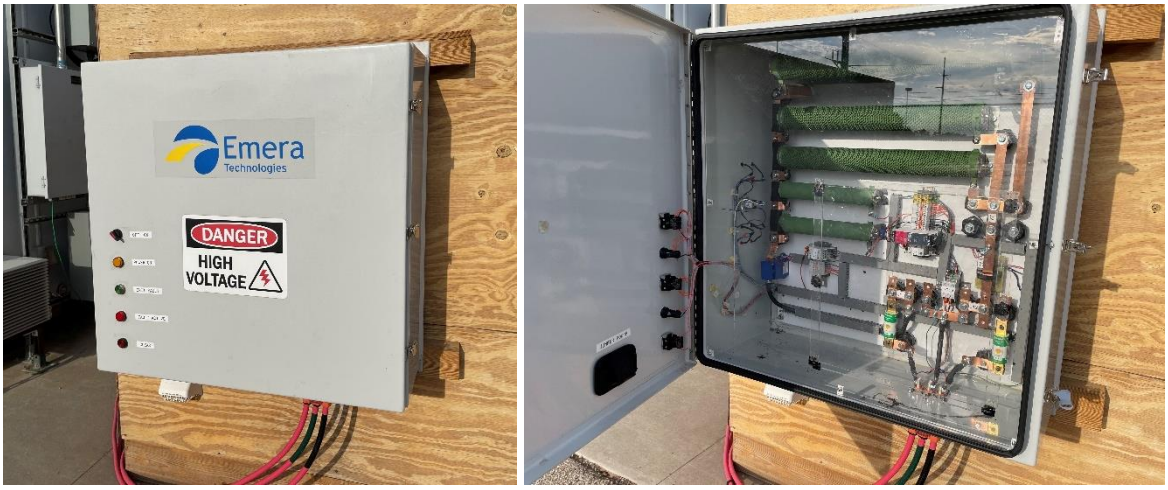

Fig. 6. Fault emulator hardware installed onto microgrid distribution bus at the DETL.

Observing the fault signatures at various locations is achieved by using oscilloscopes connecting to voltage probes and current transducers installed onto the microgrid distribution bus. Tektronix P5200A differential voltage probes and Danisense DS50UB-10V (50 A version) or DS600UB-10V (600 A version) current transducers were chosen for their high signal bandwidth, high measurement range, and accuracy for fault capture. The sensors and transducers are connected to a TBS2104B oscilloscope to capture transient waveforms during the fault initiation using a 20 MHz sampling rate over a 1 second sampling window. While voltage probes are connected directly at the point of measurement, the current transducers can be positioned on the distribution bus to monitor currents flowing to either the fault, the CEP, or into an individual nanogrid box, allowing for more understanding of how fault currents are distributed through a system.

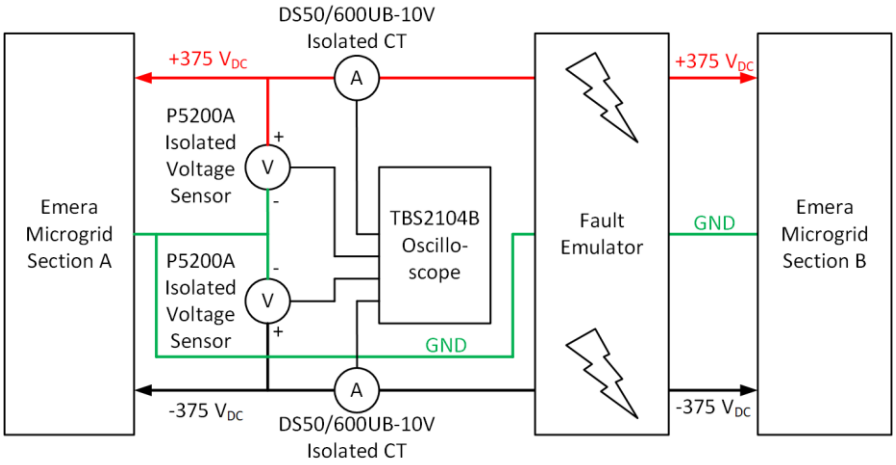

Fig. 7. Experimental fault test setup with measurement equipment connected to sections of the microgrid.

As mentioned, there are many sets of test parameters that can be considered on the microgrid, generating a large combination of potential scenarios that can be considered for this study:

- Fault impedances of 1 Ω, 4.7 Ω, 500 Ω, 1000 Ω.
- Fault connection between +375 V to ground, -375 V to ground, +375 V to -375 V.
- Fault emulator located at the DETL, near KAFB housing, or CEP.
- Measurement equipment located at the DETL, near KAFB, or CEP.
- Bus topology set for radial feed or loop feed configurations.

For the experimental results section, the following scenarios are captured. These offer observations as to the impact of fault events on the microgrid and the influence of the CEP's protection device on the microgrid.

- Fault impedance of 4.7 Ω between +375V and -375 V located at the Gathering Space, measured at the CEP with the bus topology set to a radial feed (see Fig. 4).
- Fault impedance of 1 Ω between +375V and ground located at DETL, measured at DETL and the CEP with the bus topology set to a loop feed (see Fig. 5).

The next section captures results for the two fault scenarios, detailing some of the observations that can be made from testing. Many more iterations of fault emulation are possible though the work in this paper focused on the fault results for both a low impedance fault between distribution voltages that enable the protection device and a ground fault that demonstrates the effect of connecting to the high-impedance grounding scheme.

EXPERIMENTAL FAULT TEST RESULTS

4.7 Ω Line-to-Line Fault in a Radial Feed Configuration

Results capture for a 4.7 Ω bus fault between the +375 V and -375 V distribution lines are shown below. In this scenario, the fault emulator was placed at the KAFB Gathering Space and measurements were captured at three different places on the microgrid: at the fault, at the DETL's nanogrid box, and at the CEP's community box. For each measurement location, a voltage waveform transition is used to trigger the oscilloscope capture (positive line voltage to ground measurements shown in Fig. 8. A few key observations can be made from this data. For one, the transient current is found to be significant at the point of the fault emulator with a peak transient current into the fault of 150 A. This is due to the low impedance of the fault (4.7 Ω) in relation to the line-to-line bus voltage of 750 V. When the fault is applied, current contributions from each of the nodes on the microgrid are immediately sunk into the fault emulator's power resistors. The bus voltage does see an instantaneous undershoot transient at 0 seconds, recovering momentarily before the protection device detects the overcurrent event and discharges the distribution bus. Oscillations are seen during the protection device's disabling of the distribution bus, the effect of discharging the bus capacitance of the system and the line inductance between each nanogrid and the CEP. Additionally, during the activation of the protection device, the positive line voltage can be seen inverting its polarity to ground, an effect of fault-current limiting inductances and the internal IGBT device used to shunt the line energy to ground. During this discharge, a reduction in the overall peak current into the fault is observed in relation to the reduction in overall bus voltage. While the instantaneous current on the bus is found to be significant, the protection device functions at detecting and discharging the fault within 1 millisecond, providing a fast correction to a potentially dangerous fault condition. After the fault is detected and cleared, the distribution bus is held at 0 V until the fault can be removed, and the bus can be re-enabled.

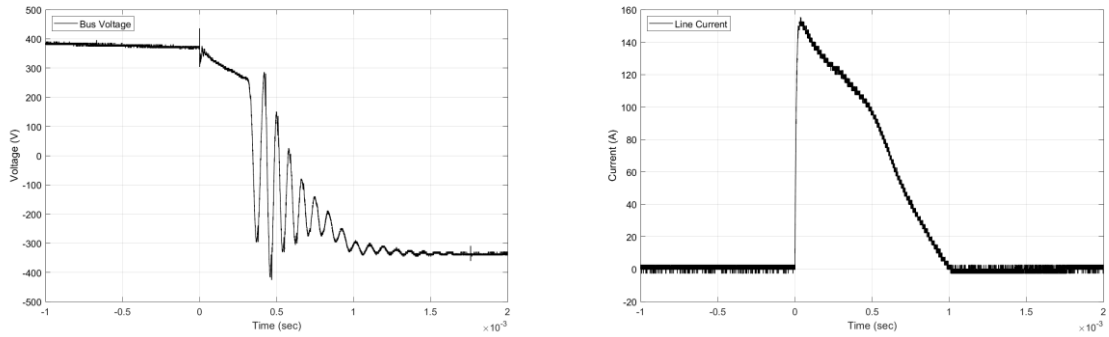

Fig. 8. Experimental fault test results for a 4.7 Ω line-to-line fault captured at the fault location (Gathering Space).

Measuring the fault event from the vantage point of the laboratory facility (DETL) nanogrid box looking towards the fault location shows a different fault signature. Fig. 9 details a more subdued oscillation on the voltage bus during fault and different oscillations between the voltage and current during the fault event. Fault currents were still significant but are contained within 2 milliseconds through the enabling of the protection device.

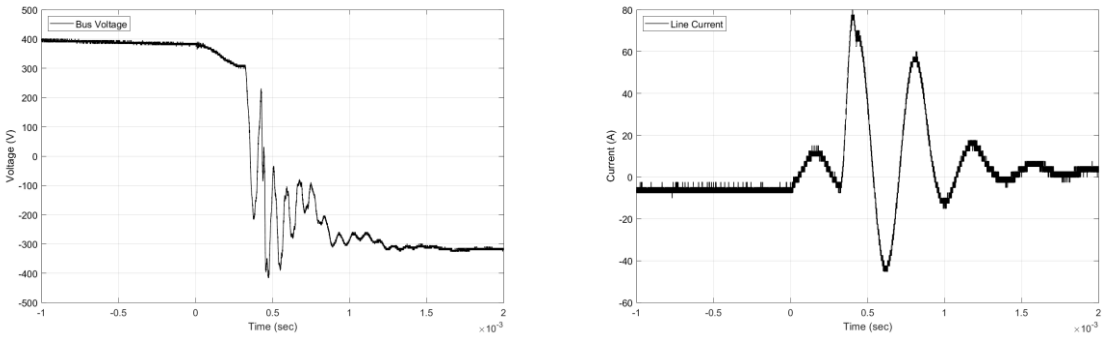

Fig. 9. Experimental fault test results for a 4.7 Ω line-to-line fault captured at the DETL's nanogrid box (NG9).

Last observed is the fault behavior seen at the CEP location shown in Fig. 10, containing the protection device used to detect and disable faults on the microgrid distribution bus. The current fed out of the CEP shows an increase to 60A before the protection device is enabled and bus current is immediately discharged back into the protection device at a peak level of up to -150 A. The bus voltage shows a fast discharge once the protection device is enabled and less ringing due to the proximity of the measured location to the protection device. The current fed back into the CEP is dissipated in the protection device rather than being fed into its local energy storage or utility grid interconnect.

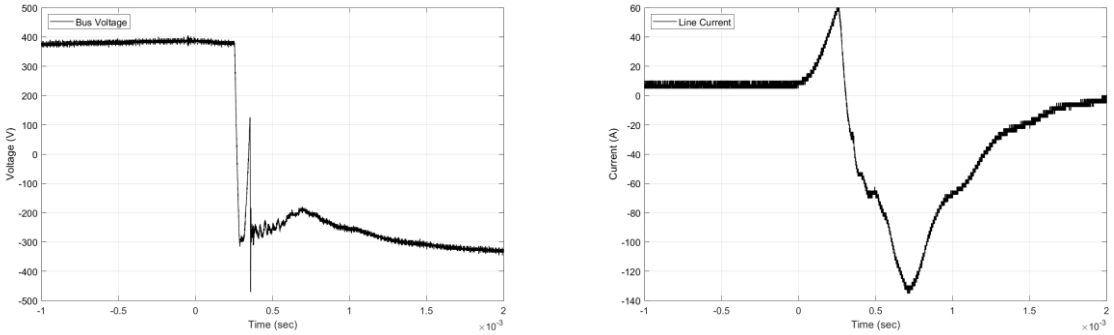

Fig. 10. Experimental fault test results for a 4.7 Ω line-to-line fault captured at the CEP (Community Box).

An additional data point captured from this test is the propagation delay found in the voltage waveforms captured during the fault. Shown below in fig. 11 are two voltage waveforms time synchronized using a GPS 1 pulse-per-second clock to align the data in post-processing. A 5 µs delay is seen when comparing the bus voltage waveform between the fault location and DETL, suggesting a delay in time between the fault occurring at the fault location and elsewhere on the distribution bus.

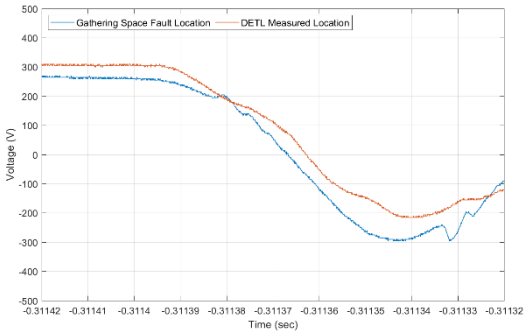

Fig. 11. Comparing time-synchronized voltage waveforms (Gathering Space, DETL) during fault event.

1 Ω Line-to-Ground Fault in a Loop Feed Configuration

Results captured for a 1 Ω fault between the +375V distribution line and ground are contained below. The fault emulator is placed at the DETL and measurements were captured at the CEP, Fig. 12, and gathering space, Fig. 13, while the microgrid was configured in a loop feed configuration. Line-to-ground provide a different fault signature than the previously detailed line-to-line faults. The ground acts as a high-impedance scheme in which the distribution bus and connected nanogrid boxes do not rely on the ground for current carrying, but rather as an earth ground connection. The fault currents at the measurement location are ultimately lower due to the high impedance of the ground with respect to the bipolar distribution bus. But the ground faults still provide some concern as the bipolar bus voltages that float between the ground can be pulled towards ground through the fault impedance. As shown in both Fig. 12 and Fig. 13, the bus voltages are pulled down during the fault to a peak minimum of -1000 V. Currents on the bus during the fault are less significant than in line-to-line faults, however can still be considered hazardous with 20 A of current detected on the line when measured at the gathering space.

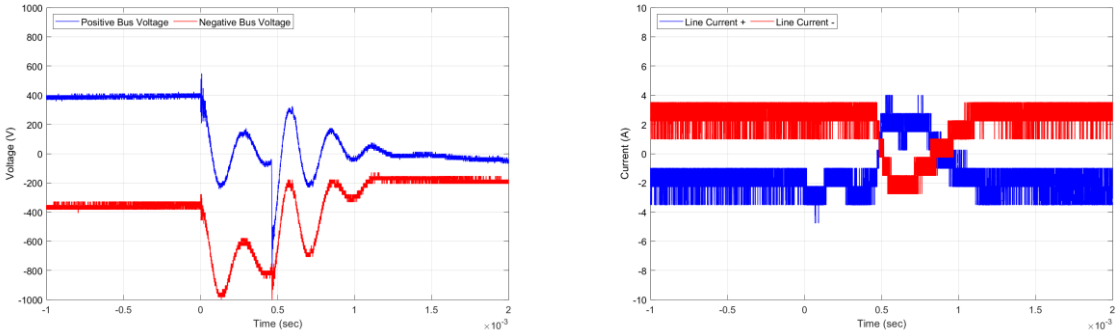

Fig. 12. Experimental fault test results for a 1 Ω +375 V to ground fault captured at the CEP (Community Box).

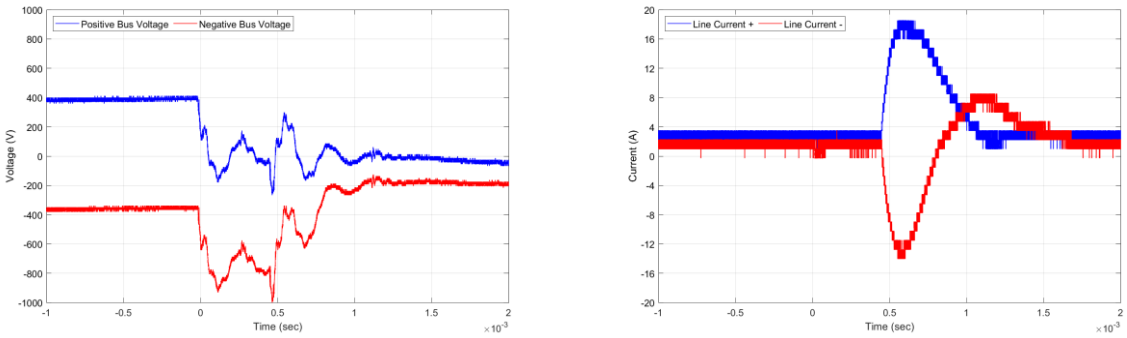

Fig. 13. Experimental fault test results for a 1 Ω +375 V to ground fault captured at the Gathering Space.

500 Ω Line-to-Ground Fault in a Loop Feed Configuration

Results captured for a 500 Ω fault between the -375V distribution line and ground are contained below. The fault emulator is placed at the DETL facility and measurements were captured at the CEP, gathering space, and fault location while the microgrid was configured in a loop feed configuration.

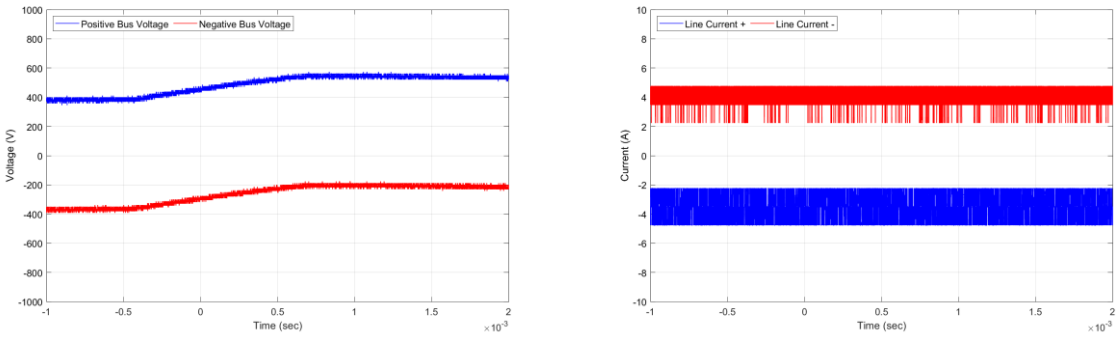

Fig. 14. Experimental fault test results for a 500 Ω -375 V-to-ground fault captured at the CEP (Community Box).

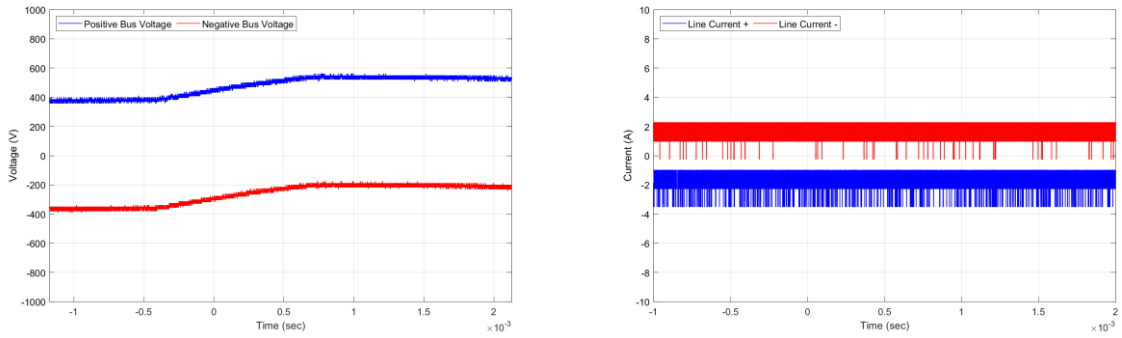

Fig. 15. Experimental fault test results for a 500 Ω -375V to ground fault captured at the Gathering Space.

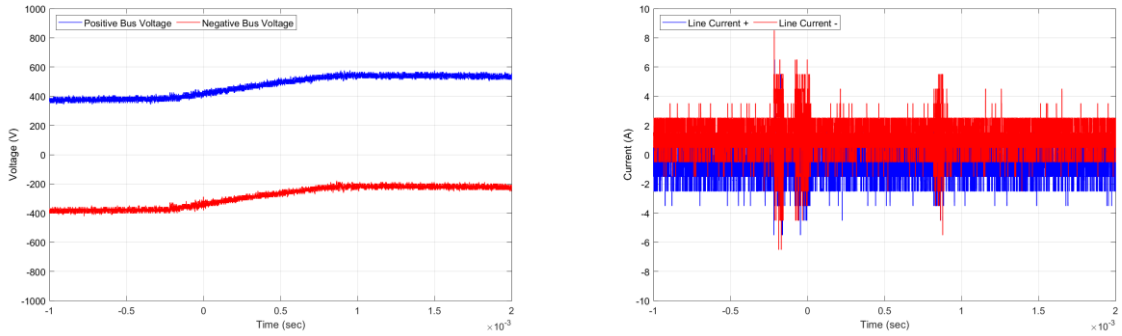

Fig. 16. Experimental fault test results for a 500 Ω -375V to ground fault captured at the DETL (fault location).

The results show a less severe fluctuation in voltage, namely due to the high impedance of the fault. Fault currents are not shown to be significant, however these faults can be concerning due to the shift in voltage and flow of current through the fault impedance into the earth ground connection. This can lead to imbalances in the bipolar bus, in this scenario showing these voltages to shift both positive and negative poles with respect to ground, the positive bus floating up to +600 V and the negative bus up to -200 V. The only substantial fault currents that could be seen during this scenario occur at the fault, though within 5 A. These faults present a concern as they are much more difficult to detect yet can have impact on the distribution bus behavior.

CONCLUSION

This work covers the test capability established on the KAFB DC microgrid for emulating fault behavior on the microgrid's distribution line as a means of better understanding hazardous electrical faults on a power distribution system. The faults are captured by monitoring the line voltage and current behavior at various locations during the controlled fault event, involving the insertion of resistance between the two distribution bus voltages or bus voltage to ground. The fault test setup can measure transient waveforms using an oscilloscope, differential voltage probes, and bidirectional current transducers that can monitor the distribution line's high current and voltage transients during the fault event. Captured results show the significant energy found during a line-to-line fault event at low impedance, exemplifying the concern that fault events can have for power systems. With high current and voltage transients during fault events, potential harm can occur due to the high amount of energy present. The results for the KAFB microgrid show promise in the integration of a fault protection device that detects significant fault events and disables the bus within 1 millisecond upon fault detection. Higher impedance faults are shown to be less significant in voltage and current transients, therefore more concerning and challenging as it relates to fault detection. Faults are continued to be studied in this experimental setup to provide better fault detection methods and understanding as it relates to DC microgrids and power distribution systems.

BIBLIOGRAPHY

[1] S. Hall, “Home Structure Fires”, NFPA Research, 2023.

[2] D. Ton, “Kirtland Air Force Base DC Microgrid is Fully Operational”, Department of Energy, Office of Electricity, 2020.

[3] J. -D. Park and J. Candelaria, "Fault Detection and Isolation in Low-Voltage DC-Bus Microgrid System," in IEEE Transactions on Power Delivery, vol. 28, no. 2, pp. 779-787, April 2013.

[4] M. Sharanya, M. Meenakshi Devi and M. Geethanjali, "Fault Detection and Location in DC Microgrid," 2018 National Power Engineering Conference (NPEC), Madurai, India, 2018, pp. 1-7.

[5] N. K. Sharma, R. Pattanayak, S. R. Samantaray and C. N. Bhende, "A Fast Fault Detection Scheme for Low Voltage DC Microgrid," 2020 21st National Power Systems Conference (NPSC), Gandhinagar, India, 2020.

[6] G. Madingou, M. Zarghami and M. Vaziri, "Fault detection and isolation in a DC microgrid using a central processing unit," 2015 IEEE Power & Energy Society Innovative Smart Grid Technologies Conference (ISGT), Washington, DC, USA, 2015

[7] R. Darbali-Zamora, A. R. R. Dow, F. Palacios, J. D. Flicker and D. Bauer, "Development of a State-Space Average Nanogrid Model for DC Microgrid Power Management Applications," 2023 IEEE Power & Energy Society Innovative Smart Grid Technologies Conference (ISGT), Washington, DC, USA, 2023.

[8] L. Zubieta, Y. Zhang and D. Bauer, "Protection Scheme for a Residential DC Microgrid," 2021 IEEE Fourth International Conference on DC Microgrids (ICDCM), Arlington, VA, USA, 2021.

[9] Pires, Vitor Fernão, Armando Pires, and Armando Cordeiro. 2023. "DC Microgrids: Benefits, Architectures, Perspectives and Challenges" Energies 16, no. 3: 1217.

[10] S. T. Ojetola and M. J. Reno, “Time Series Classification for Detecting Fault Location in a DC Microgrid”, IEEE PES Grid Edge Technologies Conference & Exposition, 2023.

[11] J. Hernandez-Alvidrez, A. R. R. Dow, M. Jimenez-Aparicio, M. J. Reno, D. Bauer, and D. Ruiz, “Field Validation of a Local, Traveling-Wave, Fault Detection Method for DC Microgrids”, IEEE Innovation Smart Grid Technologies Latin America (ISGT LA), 2023.

[12] S. Paruthiyil, A. Bidram, M. Jimenez Aparicio, J. Hernandez, and M. J. Reno, “Hardware Implementation of a Traveling Wave Protection Device for DC Microgrids” IEEE Kansas Power & Energy Conference (KPEC), 2023.

[13] R. Montoya, B. Poudel, A. Bidram, M. J. Reno, “DC Microgrid Fault Detection Using Multiresolution Analysis of Traveling Waves,” International Journal of Electric Power & Energy Systems, 2022.